**EGFR Down-regulation After anti-EGFR Therapy Predicts the Anti-tumor Effect in Colorectal Cancer**

Yasuyuki Okada[1], Tetsuo Kimura[1], Tadahiko Nakagawa[1], Koichi Okamoto[1], Akira Fukuya[1], Takahiro Goji[1], Shota Fujimoto[1], Masahiro Sogabe[2], Hiroshi Miyamoto[1], Naoki Muguruma[1], Yasushi Tsuji[3], Toshiya Okahisa[2], Tetsuji Takayama[1].

1) Department of Gastroenterology and Oncology, Institute of Biomedical Sciences, Tokushima University Graduate School,
   3-18-15 Kuramoto-cho, Tokushima, 770-8503, Japan.
2) Department of General Medicine and Community Health Science, Institute of Biomedical Sciences, Tokushima University Graduate School,
   3-18-15 Kuramoto-cho, Tokushima, 770-8503, Japan.
3) Department of Medical Oncology, Tonan Hospital, North-1, West-6, Chuo-ku, Sapporo, 060-0001, Japan.

**Running Title**: EGFR Down-regulation Predicts anti-EGFR Response

**Key words:** colorectal cancer, EGFR, internalization, degradation, cetuximab

**Corresponding author:**

Tetsuji Takayama,

Department of Gastroenterology and Oncology, Institute of Biomedical Sciences,

Tokushima University Graduate School,

3-18-15, Kuramoto-cho, Tokushima city, 770-8503, Japan

Tel: +81-88-633-7124/Fax: +81-88-633-9235/e-mail: takayama@tokushima-u.ac.jp

**Conflict of Interest**

The authors declare no conflict of interest.

**Abbreviations list:**

ABC, antibody-binding capacity; ADCC, antibody-dependent cellular cytotoxicity; ATCC, American Type Culture Collection; BSA, bovine serum albumin; CR, complete response; CRC, colorectal cancer; CT, computed tomography; ECACC, European Collection of Authenticated Cell Cultures; EGF, epidermal growth factor; EGFR, epidermal growth factor receptor; ETS, early tumor shrinkage; FBS, fetal bovine serum; FISH, fluorescent in situ hybridization; HRP, horseradish peroxidase; HSRRB, Health Science Research Resources Bank; IHC, immunohistochemistry; MesNa, Mercaptoethanesulfonic acid sodium; mCRC, metastatic colorectal cancer; mAb, monoclonal antibody; mAbs, monoclonal antibodies; PARP, poly (ADP-ribose) polymerase; PBS, phosphate buffered saline; PD, progressive disease; p-ERK, phosphorylated ERK; PNA-LNA, peptide nucleic acid-locked nucleic acid; PR, partial response; PVDF, polyvinylidene difluoride; RECIST, Response Evaluation Criteria in Solid Tumors; RIKEN BRC, RIKEN BioResource Center; SD, stable disease; SDS, sodium dodecyl sulfate; SDS-PAGE, SDS-polyamide gel electrophoresis; TBS-T, Tris-buffered saline with 0.1% Tween; TGF-α, transforming growth factor-α.

**Abstract**

Anti-epidermal growth factor receptor (EGFR) monoclonal antibody (mAb) is reported to induce EGFR internalization in colorectal cancer (CRC) cells. However, the biological relevance of EGFR internalization with anti-EGFR mAb is unknown. Therefore, the relevance of EGFR downregulation with anti-EGFR mAb to anti-tumor activity in CRC cells was investigated. Quantification of EGFR on the cell surface before cetuximab treatment was assessed by flow cytometry, and its growth-inhibitory effects were measured by trypan blue-exclusion, in 10 *RAS*, *BRAF* wild-type CRC cell lines, but there was no significant correlation between EGFR number and its growth-inhibitory effect. However, a significant correlation existed between the percentage decrease in the number of EGFRs after cetuximab treatment and its growth-inhibitory effect in those cell lines. Treatment with TGF-α, a ligand for EGFR, induced EGFR internalization in CRC cells, but most EGFRs subsequently recycled to the cell surface, consistent with previous studies. While cetuximab treatment induced EGFR internalization, most receptors subsequently translocated into the late endosome, leading to lysosomal degradation, as revealed by immunoblotting and double immunofluorescence. Cetuximab-sensitive CRC cells showed greater EGFR internalization, stronger cell growth inhibition, and more augmented apoptotic signals than non-sensitive cells. Immunohistochemistry (IHC) for EGFR, performed using an EGFR pharmDx™kit (mouse

anti-human EGFR mAb clone 2-18C9), in clinical specimens before and after anti-EGFR mAb therapy in 13 CRC patients showed a significant correlation between the response to anti-EGFR mAb and decreased staining after therapy.

**Implications:** This report clearly demonstrates that anti-EGFR mAb facilitates internalization and subsequent degradation of EGFRs in lysosomes, which is an important determinant of the efficacy of anti-EGFR mAb treatment for CRC.

## Introduction

Epidermal growth factor receptor (EGFR) represents a unique target in cancer therapy because overexpression of EGFRs has been implicated in the pathogenesis of many malignant tumors, such as head and neck cancer, colorectal cancer (CRC), lung cancer, ovarian cancer, cervical cancer, and gastric cancer (1-6). There are two therapeutic strategies targeting EGFRs: monoclonal antibodies (mAbs) and tyrosine kinase inhibitors against EGFR. While kinase inhibitors bind to the intracellular domain of the EGFR and block kinase activity, antibodies target the extracellular part of the receptor, thereby preventing ligand binding, conformational activation, and/or receptor dimerization (7-9). For patients with metastatic CRC (mCRC), two mAbs targeting EGFR, cetuximab and panitumumab, have been proven to be effective in combination with chemotherapy or as monotherapy (10-15). However, recently it has been shown that these drugs are ineffective in CRCs with *RAS* mutation, which causes constant oncogenic activation of RAS/MEK/ERK signal transduction at the EGFR downstream. Thus, *RAS* mutation is the only established biomarker for selection of patients with mCRC. Moreover, numerous studies have investigated the association of EGFR molecular events with the response to EGFR mAbs and have demonstrated that the levels of expression or somatic mutations of EGFR did not correlate with clinical responses to cetuximab and panitumumab. Thus, the response to EGFR mAbs varies among individuals

and cannot be universally expected even in the *RAS* wild-type mCRC, which presents a significant problem in clinical practice.

Anti-EGFR mAbs bind to domain III of the EGFR and inhibit binding of activating ligands (16). They also have a cytotoxic effect by inducing antibody-dependent cellular cytotoxicity (ADCC) and can counteract tumor growth through several different mechanisms (17). One important mechanism to counteract cancer cell proliferation is induction of receptor internalization and downregulation. The mouse anti-EGFR mAb (clone 225) has been shown to induce endocytosis of the EGFR (18,19). However, antibody-dependent EGFR dynamics are very complex, and the mechanism and pattern of cetuximab-induced downregulation of EGFR in CRC is not fully understood. Moreover, it is unclear whether antibody-induced EGFR internalization is related to the antibody's biological activity. Therefore, we have in the current study investigated how antibody-induced EGFR downregulation is associated with anti-tumor activity in CRC cells. Our results suggest that the degree of EGFR degradation is a more important determinant of cetuximab treatment efficacy than the initial number of EGFRs on the cell surface. Furthermore, we demonstrated that cetuximab binding to EGFR augments EGFR downregulation due to its translocalization to the late endosome, leading to lysosomal degradation. These studies provide new clinical insight into the mechanism of responsiveness to anti-EGFR antibody therapy.

## Materials and Methods

### Cell culture and reagents

We used 22 CRC cell lines. Of these, CoCM-1, COLO201, COLO320DM, CCK-81, DLD-1, and OUMS-23 cell lines were purchased from the Health Science Research Resources Bank (HSRRB, Tokyo, Japan). Caco-2, HCT116, HT29, LS174T, SW48, SW480, SW1417, and T84 cell lines were purchased from the American Type Culture Collection (ATCC, Manassas, VA). HCA-7, HCA-46, LIM1215, and HT55 cell lines were obtained from the European Collection of Authenticated Cell Cultures (ECACC, Salisbury, Wilshire, UK). COLO205, JHCOLOYI and PMF-ko14 were obtained from RIKEN BioResource Center (RIKEN BRC, Ibaraki, Japan). The M7609 cell line was kindly provided by Dr. R. Machida (Hirosaki University, Hirosaki, Japan). All cell lines were originally received from 2009 to 2014 and authenticated by short tandem repeat assay at BEX Co., Ltd (Tokyo, Japan) in 2016. No specific authentication of the M7609 cell line was performed. All cell lines were cultured in recommended media supplemented with fetal bovine serum (FBS) at 37 °C with $CO_2$, as described in Supplementary Table S1. Cetuximab was purchased from Merck Co., Ltd. (Darmstadt, Germany). A recombinant human epidermal growth factor (EGF) was obtained from Pepro Tech Inc. (Rocky Hill, NJ). Recombinant human transforming growth factor-α (TGF-α) and amphiregulin were obtained from Wako Co., Ltd. (Tokyo, Japan).

2-Mercaptoethanesulfonic acid sodium (MesNa) and iodoacetamide were obtained from Sigma-Aldrich (St Louis, MO).

**Mutational analyses of *KRAS*, *NRAS*, *BRAF*, *PIK3CA*, and *EGFR***

Genomic DNA was extracted from each cell line using a QIAamp Mini kit (Qiagen, Hilden, Germany) according to the manufacturer's instructions. *KRAS* (codon 12, 13) and *BRAF* (codon 600) and EGFR ectodomain (exon 12) mutations were detected by direct sequencing using an ABI PRISM® 3100 Genetic Analyzer (Applied Biosystems, Hitachi, Japan). Mutations in *KRAS* (codons 61, 146), *NRAS* (codons 12, 13, 61), and *PIK3CA* (codon 1047) were detected by Luminex assay. We excluded *PIK3CA* codon 542, 545, and 546 mutational analysis because it has already been shown that they have no significant effect on the response to cetuximab treatment (20). Mutations in the intracellular domain of EGFR were detected by the peptide nucleic acid-locked nucleic acid (PNA-LNA) PCR clamp method (21,22). This technique detects several EGFR mutations including G719S, G719C, G719A, T790M, L858R, L861Q, and exon 19 deletions.

**Cell viability assay**

Cell viability was determined using the trypan blue dye exclusion method. Each cell line ($1.0 \times 10^5$ cells) was plated in a 6-well plate and incubated in medium with 10% FBS in the presence of cetuximab (30 nM) or vehicle only. Viable cells were counted at day 4 and day 7 using a Countess II automated cell counter (Thermo Fisher Scientific, Inc., Waltham, MA). The growth inhibition rate was calculated as the ratio of the cell number in the presence of cetuximab to that in the presence of vehicle only.

**Quantification of cell surface EGFR by flow cytometry**

Cells were washed and then detached using trypsin and EDTA at 37 °C. Trypsin was inactivated by adding a soybean trypsin inhibitor (Wako). The cells were then incubated with mouse anti-human EGFR monoclonal antibody (sc-120, Santa Cruz Biotechnology, Inc., Santa Cruz, CA) on ice for 45 minutes. After washing the cells 3 times with 10 mM phosphate buffered saline (PBS) supplemented with 0.1% bovine serum albumin (BSA), they were further incubated with 100 μl of FITC-conjugated F(ab')2 fragment of goat anti-mouse IgG polyclonal antibody (Dako, Glostrup, Denmark) in the dark on ice for 45 minutes. The staining of cells with mAb were analyzed using a Beckman Coulter EPICS XL-MCL Flow Cytometer (Beckman Coulter, Krefeld, Germany). Quantification of EGFR on the cell surface was performed using Dako QIFKIT® (Dako) according to the manufacturer's instructions.

Briefly, 5 populations of calibration beads, bearing different numbers of mAb molecules, were analyzed by flow cytometry. The mean fluorescence intensity of each population of beads was used for construction of a calibration curve for antibody-binding capacity (ABC). The ABC of the cells analyzed by flow cytometry was calculated by interpolation from the calibration curve.

**Western blot analysis**

Cells were rinsed in cold PBS and lysed in lysis buffer (50 mM Tris-HCl, pH 8.0, 150 mM sodium chloride, 1.0% NP-40, 0.5% sodium deoxycholate, and 0.1% sodium dodecyl sulfate [SDS]). Total protein concentration in the lysates was determined using a BCA protein assay kit (Thermo Fisher Scientific Inc., Waltham, MA). Protein lysates were subjected to SDS-polyamide gel electrophoresis (SDS-PAGE) and then transferred to a polyvinylidene difluoride (PVDF) membrane. After blocking using 5% fat-free dry milk in Tris-buffered saline with 0.1% Tween (TBS-T) for 1 hour at room temperature, the membranes were probed with rabbit anti-human EGFR polyclonal antibody (sc-03, Santa Cruz Biotechnology, Inc.), rabbit anti-human ERK polyclonal antibody (sc-94, Santa Cruz Biotechnology, Inc.), rabbit anti-human phosphorylated ERK (p-ERK) monoclonal antibody (#4377, Cell Signaling Technology, Tokyo, Japan), or rabbit anti-human PARP polyclonal

antibody (#9542, Cell Signaling Technology) at 4 °C overnight. The membranes were then washed with TBS-T and incubated with the corresponding secondary horseradish-conjugated goat anti-rabbit antibodies (GE Healthcare UK, Ltd., Buckinghamshire, UK) at room temperature for 1 hour. After washing in TBS-T, the immunoblots were visualized using ECL detection reagents (GE Healthcare UK, Ltd). β-actin (Sigma-Aldrich) was used as a loading control.

**Biotinylation Assay**

Cells were serum-starved for 24 hours prior to the assay, washed with ice-cold PBS twice, and incubated with 0.5 mg/ml biotin (EZ-link Sulfo-NHS-SS-Biotin, Thermo Scientific) for 30 minutes at 4 °C. Subsequently, biotin was quenched with 50 mM $NH_4Cl$. Cells were then scraped gently, rinsed with TBS, and lysed with lysis buffer (50 mM Tris-HCl, pH 8.0, 150 mM sodium chloride, 1.0% NP-40, 0.5% sodium deoxycholate, and 0.1% SDS). Equal amount of protein was added to 500 μL of 50% streptavidin-agarose beads (NeutrAvidin Agarose Resin, Thermo Scientific) and incubated for 60 minutes at room temperature. The beads were then rinsed with wash buffer 3 times and incubated with 50 mM DTT to cleave disulfide bonds in avidin-biotin-labeled protein. Protein was eluted with SDS-PAGE sample buffer and subjected to Western blot analyses.

**Biotinylation-based EGFR internalization assay**

CCK-81 and Caco-2 cells were serum-starved for 24 hours prior to the assay and washed in ice-cold PBS twice. Surface proteins were then biotinylated with 0.5 mg/ml sulfo-NHS-SS-biotin for 30 minutes at 4 °C, followed by washing with TBS and placement on ice. For internalization, cells were incubated in pre-warmed MEM containing 30 nM cetuximab at 37 °C for 10 minutes, whereas the control cells were incubated with vehicle alone. Surface biotin was then stripped from the cells with a 10 minutes incubation in 50 mM MesNa in TBS, followed by washing and quenching MesNa with 20 mM iodoacetamide in TBS for 10 minutes. The cells were subsequently lysed, precipitated with 50% streptavidin-agarose beads, and subjected to Western blot analyses.

**Double immunofluorescence**

Cells were fixed with 4% paraformaldehyde for 30 minutes and permeabilized with 0.25% Triton X-100 in PBS for 5 minutes. After blocking using 5% BSA in PBS with 0.03% Triton X-100 for 1 hour at room temperature, the cells were incubated with anti-EGFR Alexa Fluor® 488-conjugated rabbit monoclonal antibody (#5616, Cell Signaling Technology) and anti-LAMP-1 Alexa Fluor® 647-conjugated mouse monoclonal antibody (H4A3, BioLegend,

Inc., San Diego, CA) for 2 hours at room temperature. Cells were then washed thoroughly with PBS and mounted with Prolong® Gold antifade reagent with DAPI (Thermo Fisher Scientific Inc.). Fluorescent images were obtained using a Nikon A1 confocal microscope (Nikon Corporation, Tokyo, Japan).

**Patients**

Thirteen patients with CRC whose tissues were available before and after anti-EGFR mAb treatment by surgical resection or endoscopic biopsies were enrolled. Baseline characteristics of the patients are shown in Table 1. The cohort consisted of 10 men and 3 women, with a median age of 59 years (range 36 – 72 years). Of the 13 patients, 9 were treated with cetuximab-containing therapy and 4 with panitumumab-containing therapy. Four patients had received prior treatment. The median time from the last dose of anti-EGFR mAbs to acquisition of tissue was 27 days. The response to anti-EGFR therapy was evaluated by computed tomography (CT) according to the Response Evaluation Criteria in Solid Tumors (RECIST; version 1.1). Patients were classified as either responders (confirmed complete response [CR], or partial response [PR]) or non-responders (stable disease [SD] or progressive disease [PD]) based on the best response evaluated by RECIST. The present study

was approved by the Institutional Review Board of Tokushima University Hospital and informed consent was obtained from all patients.

**Immunohistochemistry (IHC)**

Immunohistochemical staining for EGFR in CRC tissue was performed using an EGFR pharmDx™ kit (Dako) according to the manufacturer's instructions. Briefly, 4-μm paraffin-embedded tissue sections were deparaffinized, incubated with proteinase K solution, and treated with 3% $H_2O_2$ to block endogenous peroxidase. They were then incubated with a mouse anti-human EGFR mAb (clone 2-18C9) at 4 °C overnight. They were washed with PBS and incubated with horseradish peroxidase (HRP)-conjugated polymers at room temperature for 30 minutes, followed by visualization with DAB (3, 3'-diaminobenzidine tetrahydrochloride). Finally, the slides were counterstained with hematoxylin.

Positive staining was evaluated and classified based on IHC scores (0, 1, 2 or 3) according to the percentage of positive cells and staining intensity, as described by Chung and colleagues with a minor modification (23). The IHC score designations were as follows: 0, no membranous staining in any tumor cells; 1, staining of less than 10% of tumor cells with any intensity or in less than 30% of tumor cells with weak intensity; 2, staining in 10% to 30% of tumor cells with moderate to strong intensity or staining in 30% to 50% of tumor cells with

weak to moderate intensity; and 3, staining in more than 30% of tumor cells with strong intensity or more than 50% of tumor cells with any intensity. Immunoreactivity was evaluated independently by 2 investigators (Y.O. and T.T). Cases with discrepancies were jointly reevaluated and a consensus was reached. Changes in IHC scores before and after treatment were then categorized into 3 groups; “no change” showing the same IHC scores before and after treatment, “moderate decrease” showing a 1 scale reduction after treatment, and “marked decrease” showing more than a 2 scale reduction after treatment.

## Results

### Growth-inhibitory effect of cetuximab differs in the various *RAS, RAF* wild-type CRC cell lines

Among the 22 CRC cell lines examined, 10 cell lines (CoCM-1, COLO320DM, CCK-81, Caco-2, HCA-7, HCA-46, LIM1215, HT55, PMF-ko14, and JHCOLOYI) were both *KRAS* (codon 12, 13) wild-type and *BRAF* wild-type (Supplementary Table S2). Moreover, we analyzed the mutation status of *KRAS* (codons 61 and 146), *NRAS* (codons 12, 13 and 61), *PIK3CA* (codon 1047), and *EGFR* (exon 12 and exon 18-21) in these 10 cell lines and confirmed that there were no mutations in these genes. We then evaluated the inhibitory effect of cetuximab on cell growth in these 10 *RAS, RAF* wild-type CRC cell lines (Figure 1). The growth of CCK-81, LIM-1215, and HCA-7 cell lines was inhibited by more than 80% at 7 days after cetuximab treatment. Conversely, the growth of COLO320DM and PMF-ko14 was negligibly inhibited by cetuximab treatment. The remaining cell lines showed approximately 30% to 70% inhibition of cell growth at 7 days after cetuximab treatment. Thus, the growth-inhibitory effect of cetuximab varied even among *RAS, RAF* wild-type cell lines. These results are consistent with clinical findings that the response to cetuximab differs even among cancers with no mutation in the EGFR signaling pathway.

**Decrease in cell surface EGFRs correlates with the anti-tumor activity of cetuximab**

To assess the relationship between the number of EGFRs and the efficacy of cetuximab, we measured the number of EGFRs on the cell surface by flow cytometry in the 10 cell lines before and after addition of cetuximab (Figure 2A). The initial number of EGFRs on the cell surface varied among the cell lines. HCA-7, PMF-ko14, and LIM-1215 cells had more than 20,000 EGFRs per cell, whereas JHCOLOYI and COLO320DM cells had less than 1,000 per cell. After addition of cetuximab, the number of EGFRs on the cell surface decreased in all cell lines due to cetuximab-induced internalization of EGFR. However, the degree of EGFR internalization varied among the cell lines. When we compared the initial number of EGFRs on the cell surface with the growth-inhibitory effect of cetuximab, no significant relationship was observed ($p$=0.141) (Figure 2B). However, the percentage decrease in the number of EGFRs correlated significantly with the degree of growth inhibition by cetuximab ($p$=0.040) (Figure 2C), suggesting that the degree of EGFR internalization correlates with the response to anti-EGFR treatment.

**Cetuximab induces EGFR internalization and lysosomal degradation**

To clarify the mechanism by which cell surface EGFRs decreased in cetuximab-sensitive CRC cells, we first compared the binding affinity of cetuximab to cell

surface EGFR between cetuximab-sensitive and non-sensitive cell lines. However, we found no significant difference in the affinity of cetuximab for EGFR on the cell surface between cetuximab-sensitive cells and non-sensitive cells (Supplementary Figure S1). It has been reported that EGFR ligands such as EGF and TGF-α stimulate receptor internalization, leading to intracellular degradation or recycling of EGFR to the cell surface (24-26). Cetuximab, an anti-EGFR mAb, also has been reported to induce EGFR internalization, similarly to the activating ligands (18). To compare differences in EGFR trafficking after internalization, CCK-81 cells, which showed appreciable EGFR internalization with treatment, were incubated with the activating ligand TGF-α or cetuximab, and the chronological changes in EGFR numbers on the cell surface were examined. After stimulation with TGF-α, the EGFR number on the cell surface decreased by approximately 50% in 15 minutes, then close to 100% of the receptor recycled back to the cell surface, consistent with a previous report (25). After stimulation with cetuximab, however, about 80% of EGFRs were internalized, and very little EGFR was recycled back to the cell surface (Figure 3A). Interestingly, when we observed cells up to 24 hours after cetuximab treatment, a majority of the internalized EGFRs were not recycled back to the cell surface over time (Supplementary Figure S2). To extend these observations using a biotinylation approach, the cell surface proteins in CCK-81 cells treated with TGF-α or cetuximab were labeled with biotin, precipitated, and subjected to

Western blot analysis using anti-EGFR antibody. As shown in Figure 3B, levels of EGFR on the cell surface decreased 30 minutes after the addition of both activating ligand and cetuximab, indicating EGFR internalization to the cytoplasm. However, whereas cells treated with TGF-α returned most of the internalized EGFRs back to the surface, cells treated with cetuximab recycled significantly less EGFR, suggesting that the ligand and antibody have very different effects on EGFR trafficking. Moreover, although the total amount of EGFR in whole cell lysates did not change after stimulation with TGF-α, the total amount of EGFR decreased markedly over time after stimulation with cetuximab, demonstrating that the majority of cetuximab-internalized EGFR was degraded in the cells.

To confirm the degradation of EGFR in cells treated with cetuximab, the colocalization of EGFR with LAMP-1, which is located in lysosomes and helps to regulate endocytic trafficking and degradation, was examined by double immunofluorescence. Representative staining patterns are shown in Figure 3C. Before treatment with cetuximab or TGF-α, EGFR was predominantly distributed on the cell membrane of the CRC cells. After treatment with TGF-α, EGFR immunostained signal was translocated into the cytoplasm and a majority of the immunostained EGFR had not merged with LAMP-1-positive vesicles. After treatment with cetuximab, however, EGFR signal was also translocated into the cytoplasm and showed overlap with LAMP-1-positive signals. Figure 3D shows image quantification of

the merged signals of EGFR and LAMP-1. CCK-81 cells treated with cetuximab showed significantly more merged signals than cells treated with activated ligand (TGF-α). These results indicate that internalized cetuximab-EGFR complex is directed to lysosomes for degradation. Thus, it appears that, although both ligand and cetuximab induce receptor internalization, the fates of the internalized ligand-EGFR and cetuximab-EGFR complexes are different: the ligand-EGFR complex is directed to receptor recycling, but cetuximab-EGFR complex is directed to endosomal degradation.

**Cetuximab-dependent EGFR internalization correlates with decreased MAP kinase signaling**

We first observed the amount of internalized EGFR in CCK-81 (cetuximab-responsive) and Caco-2 (non-responsive) cell lines using a biotinylation-based EGFR internalization assay. As shown in Figure 4A, we confirmed EGFR internalization after treatment with cetuximab occurred more efficiently in CCK-81 cells than in Caco-2 cells. To determine whether a decrease in the number of EGFRs on the cell surface is associated with signal transduction downstream of EGFR, we investigated p-ERK and ERK expression in CCK-81 and Caco-2 cells by Western blotting after treatment with cetuximab (Figure 4B). In CCK-81 cells, which showed marked EGFR internalization, phosphorylation of ERK was

strongly inhibited by addition of cetuximab. On the other hand, Caco-2, in which EGFR was less internalized after addition of cetuximab, showed a moderate inhibitory effect of cetuximab on ERK phosphorylation. Densitometric analysis confirmed that cetuximab had a stronger inhibitory effect on the MAP kinase signaling pathway in CCK-81 than in Caco-2 cells (Figure 4C). To further investigate the induction of apoptosis in these cells, we evaluated the cleavage of poly (ADP-ribose) polymerase (PARP) by Western blotting (Figure 4D). The cleavage of PARP was markedly increased by addition of cetuximab in CCK-81 cells, but it was only faintly apparent in Caco-2 cells, indicating that apoptosis was induced to a greater extent in CCK-81 cells than in Caco-2 cells.

**EGFR degradation in CRC tissue is associated with the tumor response to anti-EGFR treatment**

To assess the clinical relevance of the *in vitro* findings, we investigated changes in EGFR expression after anti-EGFR mAb treatment in cancer tissues from 13 CRC patients in association with response to the treatment. Figure 5A shows representative staining patterns of EGFR before and after treatment: i.e., marked decrease (Case 5, Figure 5A, a-c), moderate decrease (Case 12, Figure 5A, d-f), and no change (Case 9, Figure 5A, g-i). Cancerous tissue from Case 5 showed strong EGFR staining (IHC score 3+) before treatment (Figure 5A, b),

but few signals for EGFR were seen after treatment (IHC score 0, Figure 5A, c). This case was categorized as a marked decrease. Similarly, in Case 12 EGFR was strongly stained in the majority of cancer cells before treatment (IHC score 3+), but 50% of the cells showed moderate to weak staining signals (IHC score 2+) after treatment. Thus, this case was classified as a moderate decrease. The IHC scores before and after the treatment in Case 9 were equal (IHC score 3+), so this case was categorized as no change. Out of a total of 13 cases, there was 1 case with marked decrease, 5 cases with moderate decrease, and 7 cases with no change. When we compared responders and non-responders to anti-EGFR mAb treatment, the former showed a significantly greater change in EGFR expression after treatment than did non-responders ($p<0.01$) (Figure 5B, C). This result supports the *in vitro* finding that the percentage decrease in the number of EGFRs on the cell surface correlates with the anti-tumor activity of anti-EGFR mAb and reveals a close relationship between EGFR degradation and clinical effectiveness of anti-EGFR mAb agents.

## DISCUSSION

In this study, we have shown that the degree of EGFR internalization varies in *RAS* wild-type CRC cells and is closely associated with the sensitivity to anti-EGFR antibodies. We also demonstrated that downregulation of EGFR on the cell surface after anti-EGFR antibody treatment is caused by augmented degradation of antibody-bound receptor via the endosomal-lysosomal pathway, resulting in inhibition of cell growth signals and activation of apoptotic signals. Moreover, our theory was supported by analyzing clinical samples of CRC from patients who received anti-EGFR therapy.

We did not find a significant correlation between the initial number of EGFRs on the cell surface and anti-tumor activity of cetuximab in *RAS* wild-type CRC cell lines. This result is consistent with recent clinical findings that the initial EGFR expression level is not significantly correlated with the clinical response to cetuximab and panitumumab, as revealed by IHC (11,23,27) and quantitative real-time polymerase chain reaction (28). Similarly, the result is consistent with recent studies showing no significant correlation between EGFR gene copy number and response to cetuximab, as determined by fluorescent in situ hybridization (FISH) (29,30). Interestingly, however, we found that downregulation of EGFR by anti-EGFR antibody significantly correlated with the rate of inhibition of cell proliferation. Moreover, inhibition of growth-promoting signals and activation of apoptotic signals were observed

depending on the degree of downregulation of EGFR on the surface of CRC cells. In addition, we found a significant correlation between attenuation of EGFR expression and therapeutic efficacy in cancer tissue from patients who received anti-EGFR antibody therapy. Thus, we were able to demonstrate a close correlation between EGFR downregulation in cancer tissue and efficacy of anti-EGFR antibody therapy in patients with CRC, as well as in CRC cell lines *in vitro*.

Several previous studies have investigated the mechanism of internalization and subsequent trafficking of EGFR induced by its ligands, including TGF-α and EGF (31). However, a few studies have produced contradictory results in terms of anti-EGFR antibody-induced receptor trafficking. Sunada and associates reported that 225 mAb (cetuximab) stimulated EGFR internalization and induced its downregulation to an extent comparable to that induced by ligands using the human epidermoid carcinoma cell line A431 (18). Jaramillo and coworkers reported that antibody-bound EGFR is less internalized and more recycled to the cell surface than ligand-bound EGFR in the human lung carcinoma cell lines A549, CL1-0, and CL1-5 (32). In the present study, however, we found augmented degradation of EGFR after cetuximab stimulation in the CRC cell line CCK-81. This is also supported by the fact that phosphorylation of EGFR was augmented by stimulation with ligands (TGF-α > amphiregulin) but was not augmented by treatment with cetuximab, with

respect to both cell surface protein and total protein (Supplementary Figure S3). Therefore, we next examined the localization of EGFR after antibody-induced internalization by double immunofluorescence and found that the majority of antibody-bound EGFR was indeed translocated to the late endosome after cetuximab treatment, leading to subsequent lysosomal degradation. Similar results were obtained using the CRC cell line LIM-1215 (data not shown). Moreover, results consistent with these *in vitro* findings were obtained by analyzing clinical CRC tissues before and after anti-EGFR mAb treatment. Our data demonstrate that anti-EGFR antibody efficiently induces degradation of EGFR via the endosomal/lysosomal pathway. Recently, Berger and colleagues reported a different mechanism for EGFR internalization between antibody and ligand stimulation: i.e., ligand-induced internalization was clathrin-dependent but antibody-induced internalization was clathrin-independent (33). This report also supports our theory that the localization and trafficking of antibody-bound EGFR are different from those of ligand-bound EGFR; ligand-bound EGFR is destined predominantly for recycling but antibody-bound EGFR, predominantly for lysosomal degradation. These findings are quite consistent with the data showing that EGFR downregulation is significantly correlated with the efficacy of anti-EGFR antibody treatment. Thus, our data suggest that EGFR trafficking and degradation after antibody-binding is a key mechanism of responsiveness to anti-EGFR antibody therapy.

Recently, early tumor shrinkage (ETS) and depth of response have received much attention as predictors of treatment outcomes for long-term survival (34,35). In particular, ETS has been achieved more frequently with treatment protocols that include anti-EGFR antibodies for *RAS* wild-type. The present study revealed that EGFR was rapidly downregulated in cetuximab-sensitive CRC cell lines after exposure to cetuximab, leading to strong inhibition of cell growth and enhanced apoptosis. This rapid EGFR downregulation is explained by efficient EGFR degradation in lysosomes without recycling to the cell surface. When the 13 patients with mCRC enrolled in this study were divided into ETS and non-ETS groups, there was a significant difference in EGFR downregulation by IHC (Supplementary Table S3). In this context, our results may explain the clinical phenomenon of ETS following treatment with anti-EGFR antibodies: i.e., ETS is achieved by rapid EGFR downregulation and subsequent growth inhibition and augmentation of apoptosis. ADCC is proposed as one of the mechanisms of cetuximab anti-tumor activity. ADCC activity is reportedly correlated with the absolute number of EGFRs on the cell surface, irrespective of the presence of *RAS* mutation and *RAF* mutation (36). Therefore, the correlation between the percentage decrease in the EGFR number, ADCC activity, and therapeutic effect is unclear in this study. *In vivo* experiments will be needed for a more detailed analysis.

Currently, the exact molecular mechanisms for antibody-induced EGFR downregulation have not been fully clarified. Although further investigations are needed to identify which molecules are involved in this marked degradation of EGFR, this is the first report addressing the clinical significance of EGFR degradation in anti-EGFR antibody therapy. These findings provide new insights to better understand the mechanism of action of anti-EGFR antibodies and will help to identify new positive predictors of EGFR signaling blockade.

In conclusion, downregulation of EGFRs after treatment with anti-EGFR antibody was significantly correlated with the treatment's anti-tumor activity in *RAS* wild-type CRC cell lines. Antibody-bound EGFR was efficiently degraded via the endosomal/lysosomal system, leading to inhibition of cell proliferation and augmentation of apoptosis. The correlation between EGFR downregulation and response to anti-EGFR antibodies was confirmed in patients with CRCs receiving treatment with anti-EGFR antibodies.

**Acknowledgment**

We thank Shinichiro Makimoto (Kishiwada Tokushukai Hospital, Osaka, Japan), Taisuke Matsuoka (Fukuoka Tokushukai Hospital, Fukuoka, Japan), Mayumi Kajimoto, and Yuta Higasa (Tokushima University, Tokushima, Japan) for their helpful assistance in this research.

## References


1. Nicholson RI, Gee JM, Harper ME. EGFR and cancer prognosis. Eur J Cancer **2001**;37 Suppl 4:S9-15.

2. Temam S, Kawaguchi H, El-Naggar AK, Jelinek J, Tang H, Liu DD, *et al.* Epidermal growth factor receptor copy number alterations correlate with poor clinical outcome in patients with head and neck squamous cancer. J Clin Oncol **2007**;25(16):2164-70 doi 10.1200/jco.2006.06.6605.

3. Chong CR, Janne PA. The quest to overcome resistance to EGFR-targeted therapies in cancer. Nat Med **2013**;19(11):1389-400 doi 10.1038/nm.3388.

4. Sheng Q, Liu J. The therapeutic potential of targeting the EGFR family in epithelial ovarian cancer. Br J Cancer **2011**;104(8):1241-5 doi 10.1038/bjc.2011.62.

5. Bonner JA, Harari PM, Giralt J, Cohen RB, Jones CU, Sur RK, *et al.* Radiotherapy plus cetuximab for locoregionally advanced head and neck cancer: 5-year survival data from a phase 3 randomised trial, and relation between cetuximab-induced rash and survival. Lancet Oncol **2010**;11(1):21-8 doi 10.1016/s1470-2045(09)70311-0.

6. Lordick F, Kang YK, Chung HC, Salman P, Oh SC, Bodoky G, *et al.* Capecitabine and cisplatin with or without cetuximab for patients with previously untreated advanced

gastric cancer (EXPAND): a randomised, open-label phase 3 trial. Lancet Oncol **2013**;14(6):490-9 doi 10.1016/s1470-2045(13)70102-5.

7. Hynes NE, Lane HA. ERBB receptors and cancer: the complexity of targeted inhibitors. Nat Rev Cancer **2005**;5(5):341-54 doi 10.1038/nrc1609.

8. Markman B, Capdevila J, Elez E, Tabernero J. New trends in epidermal growth factor receptor-directed monoclonal antibodies. Immunotherapy **2009**;1(6):965-82 doi 10.2217/imt.09.66.

9. Wheeler DL, Dunn EF, Harari PM. Understanding resistance to EGFR inhibitors-impact on future treatment strategies. Nat Rev Clin Oncol **2010**;7(9):493-507 doi 10.1038/nrclinonc.2010.97.

10. Van Cutsem E, Peeters M, Siena S, Humblet Y, Hendlisz A, Neyns B, *et al.* Open-label phase III trial of panitumumab plus best supportive care compared with best supportive care alone in patients with chemotherapy-refractory metastatic colorectal cancer. J Clin Oncol **2007**;25(13):1658-64 doi 10.1200/jco.2006.08.1620.

11. Cunningham D, Humblet Y, Siena S, Khayat D, Bleiberg H, Santoro A, *et al.* Cetuximab monotherapy and cetuximab plus irinotecan in irinotecan-refractory metastatic colorectal cancer. N Engl J Med **2004**;351(4):337-45 doi 10.1056/NEJMoa033025.

12. Bokemeyer C, Bondarenko I, Makhson A, Hartmann JT, Aparicio J, de Braud F, *et al.* Fluorouracil, leucovorin, and oxaliplatin with and without cetuximab in the first-line treatment of metastatic colorectal cancer. J Clin Oncol **2009**;27(5):663-71 doi 10.1200/jco.2008.20.8397.

13. Jonker DJ, O'Callaghan CJ, Karapetis CS, Zalcberg JR, Tu D, Au HJ, *et al.* Cetuximab for the treatment of colorectal cancer. N Engl J Med **2007**;357(20):2040-8 doi 10.1056/NEJMoa071834.

14. Douillard JY, Siena S, Cassidy J, Tabernero J, Burkes R, Barugel M, *et al.* Randomized, phase III trial of panitumumab with infusional fluorouracil, leucovorin, and oxaliplatin (FOLFOX4) versus FOLFOX4 alone as first-line treatment in patients with previously untreated metastatic colorectal cancer: the PRIME study. J Clin Oncol **2010**;28(31):4697-705 doi 10.1200/jco.2009.27.4860.

15. Van Cutsem E, Kohne CH, Hitre E, Zaluski J, Chang Chien CR, Makhson A, *et al.* Cetuximab and chemotherapy as initial treatment for metastatic colorectal cancer. N Engl J Med **2009**;360(14):1408-17 doi 10.1056/NEJMoa0805019.

16. Li S, Schmitz KR, Jeffrey PD, Wiltzius JJ, Kussie P, Ferguson KM. Structural basis for inhibition of the epidermal growth factor receptor by cetuximab. Cancer Cell **2005**;7(4):301-11 doi 10.1016/j.ccr.2005.03.003.

17. Vincenzi B, Zoccoli A, Pantano F, Venditti O, Galluzzo S. Cetuximab: from bench to bedside. Curr Cancer Drug Targets **2010**;10(1):80-95.

18. Sunada H, Magun BE, Mendelsohn J, MacLeod CL. Monoclonal antibody against epidermal growth factor receptor is internalized without stimulating receptor phosphorylation. Proc Natl Acad Sci U S A **1986**;83(11):3825-9.

19. Sunada H, Yu P, Peacock JS, Mendelsohn J. Modulation of tyrosine, serine, and threonine phosphorylation and intracellular processing of the epidermal growth factor receptor by antireceptor monoclonal antibody. J Cell Physiol **1990**;142(2):284-92 doi 10.1002/jcp.1041420210.

20. De Roock W, Claes B, Bernasconi D, De Schutter J, Biesmans B, Fountzilas G, *et al.* Effects of KRAS, BRAF, NRAS, and PIK3CA mutations on the efficacy of cetuximab plus chemotherapy in chemotherapy-refractory metastatic colorectal cancer: a retrospective consortium analysis. Lancet Oncol **2010**;11(8):753-62 doi 10.1016/s1470-2045(10)70130-3.

21. Nagai Y, Miyazawa H, Huqun, Tanaka T, Udagawa K, Kato M, *et al.* Genetic heterogeneity of the epidermal growth factor receptor in non-small cell lung cancer cell lines revealed by a rapid and sensitive detection system, the peptide nucleic

acid-locked nucleic acid PCR clamp. Cancer Res **2005**;65(16):7276-82 doi 10.1158/0008-5472.can-05-0331.

22. Tanaka T, Nagai Y, Miyazawa H, Koyama N, Matsuoka S, Sutani A, *et al.* Reliability of the peptide nucleic acid-locked nucleic acid polymerase chain reaction clamp-based test for epidermal growth factor receptor mutations integrated into the clinical practice for non-small cell lung cancers. Cancer Sci **2007**;98(2):246-52 doi 10.1111/j.1349-7006.2006.00377.x.

23. Chung KY, Shia J, Kemeny NE, Shah M, Schwartz GK, Tse A, *et al.* Cetuximab shows activity in colorectal cancer patients with tumors that do not express the epidermal growth factor receptor by immunohistochemistry. J Clin Oncol **2005**;23(9):1803-10 doi 10.1200/JCO.2005.08.037.

24. Henriksen L, Grandal MV, Knudsen SL, van Deurs B, Grovdal LM. Internalization mechanisms of the epidermal growth factor receptor after activation with different ligands. PLoS One **2013**;8(3):e58148 doi 10.1371/journal.pone.0058148.

25. Roepstorff K, Grandal MV, Henriksen L, Knudsen SL, Lerdrup M, Grovdal L, *et al.* Differential effects of EGFR ligands on endocytic sorting of the receptor. Traffic **2009**;10(8):1115-27 doi 10.1111/j.1600-0854.2009.00943.x.

26. Decker SJ. Epidermal growth factor and transforming growth factor-alpha induce differential processing of the epidermal growth factor receptor. Biochem Biophys Res Commun **1990**;166(2):615-21.

27. Saltz LB, Meropol NJ, Loehrer PJ, Sr., Needle MN, Kopit J, Mayer RJ. Phase II trial of cetuximab in patients with refractory colorectal cancer that expresses the epidermal growth factor receptor. J Clin Oncol **2004**;22(7):1201-8 doi 10.1200/jco.2004.10.182.

28. Vallbohmer D, Zhang W, Gordon M, Yang DY, Yun J, Press OA, *et al.* Molecular determinants of cetuximab efficacy. J Clin Oncol **2005**;23(15):3536-44 doi 10.1200/jco.2005.09.100.

29. Italiano A, Follana P, Caroli FX, Badetti JL, Benchimol D, Garnier G, *et al.* Cetuximab shows activity in colorectal cancer patients with tumors for which FISH analysis does not detect an increase in EGFR gene copy number. Ann Surg Oncol **2008**;15(2):649-54 doi 10.1245/s10434-007-9667-2.

30. Sartore-Bianchi A, Fieuws S, Veronese S, Moroni M, Personeni N, Frattini M, *et al.* Standardisation of EGFR FISH in colorectal cancer: results of an international interlaboratory reproducibility ring study. J Clin Pathol **2012**;65(3):218-23 doi 10.1136/jclinpath-2011-200353.

31. Ebner R, Derynck R. Epidermal growth factor and transforming growth factor-alpha: differential intracellular routing and processing of ligand-receptor complexes. Cell Regul **1991**;2(8):599-612.

32. Jaramillo ML, Leon Z, Grothe S, Paul-Roc B, Abulrob A, O'Connor McCourt M. Effect of the anti-receptor ligand-blocking 225 monoclonal antibody on EGF receptor endocytosis and sorting. Exp Cell Res **2006**;312(15):2778-90 doi 10.1016/j.yexcr.2006.05.008.

33. Berger C, Madshus IH, Stang E. Cetuximab in combination with anti-human IgG antibodies efficiently down-regulates the EGF receptor by macropinocytosis. Exp Cell Res **2012**;318(20):2578-91 doi 10.1016/j.yexcr.2012.09.001.

34. Piessevaux H, Buyse M, Schlichting M, Van Cutsem E, Bokemeyer C, Heeger S, *et al.* Use of early tumor shrinkage to predict long-term outcome in metastatic colorectal cancer treated with cetuximab. J Clin Oncol **2013**;31(30):3764-75 doi 10.1200/jco.2012.42.8532.

35. Heinemann V, Stintzing S, Modest DP, Giessen-Jung C, Michl M, Mansmann UR. Early tumour shrinkage (ETS) and depth of response (DpR) in the treatment of patients with metastatic colorectal cancer (mCRC). Eur J Cancer **2015**;51(14):1927-36 doi 10.1016/j.ejca.2015.06.116.

36. Seo Y, Ishii Y, Ochiai H, Fukuda K, Akimoto S, Hayashida T, *et al.* Cetuximab-mediated ADCC activity is correlated with the cell surface expression level of EGFR but not with the KRAS/BRAF mutational status in colorectal cancer. Oncol Rep **2014**;31(5):2115-22 doi 10.3892/or.2014.3077.

**Figure legends**

**Figure 1.**

Growth inhibitory curves of various *RAS, RAF* wild-type colorectal cancer (CRC) cell lines with cetuximab treatment. Each cell line was incubated with cetuximab (30 nM) or vehicle only. After 4 days and 7 days, the cells were detached and the cell number was counted using the trypan blue method. The cell-growth inhibition rate was calculated as the ratio of the number of cells treated with cetuximab to the number of cells treated with vehicle only. All experiments were performed independently at least 3 times.

**Figure 2.**

EGFR internalization induced by addition of cetuximab and its growth inhibitory effect on CRC cell lines. A) EGFR number on the cell surface before and after addition of cetuximab. After starvation for 24 hours, the cells were incubated with cetuximab (30 nM) for 7 days. Subsequently, the EGFR number was determined by flow cytometry. Values are mean ± standard deviation (SD) from 3 independent experiments. B) Correlation between cell growth inhibition rate and initial EGFR number on the cell surface (per cell). C) The correlation between the rate of cell growth inhibition and percentage decrease in EGFR number was calculated from the absolute decrease in EGFR number after addition of cetuximab divided by

the initial EGFR number. *P*-values were determined using Pearson's correlation coefficient test. $R^2$ indicates the coefficient of determination.

**Figure 3.**

EGFR ligand and cetuximab differentially affect EGFR trafficking. A) Chronological changes in the number of EGFRs on the cell surface. CCK-81 cells were incubated with TGF-α (20 nM) or cetuximab (30 nM) for 60 minutes on ice, washed, and incubated at 37 °C for different time periods. At the specified time–points, surface receptors were quantified by flow cytometry. All experiments were performed independently at least 3 times. *P*-values were determined using Student's t test. **p* <0.01. B) CCK-81 cells were incubated with TGF-α (20 nM) or cetuximab (30 nM) for 60 minutes on ice, washed, and incubated at 37 °C for different time periods. The cells were then incubated on ice with streptavidin-conjugated biotin to label cell surface proteins. Biotinylated cell surface proteins were precipitated using streptavidin-agarose beads and subjected to Western blot analysis for EGFR. Whole cell lysates for each set were also extracted and subjected to Western blot analyses. C) EGFR co-localization with LAMP-1 in CCK-81 cells. CCK-81 cells were incubated with TGF-α (20 nM) or cetuximab (30 nM) for 30 minutes and fixed in 4% paraformaldehyde. The cells were then labeled for EGFR (green) and LAMP-1 (red) as described in Materials and Methods. Bar,

10 μm. D) Quantification of the merged signal of EGFR colocalizing with LAMP-1 in cells treated with cetuximab (30 nM) or TGF-α (20 nM). Y-axis of the graph shows merged levels from an average of 5 cells for each condition. *P*-value was determined using Student's t test. *$p$ <0.01.

**Figure 4.**

Effect of cetuximab on cell growth and apoptotic signals. A) Surface proteins on CCK-81 and Caco-2 cells were biotinylated with 0.5 mg/ml streptavidin-conjugated sulfo-NHS-SS-biotin for 30 minutes at 4 °C. The cells were incubated in prewarmed MEM containing 30 nM cetuximab at 37 °C for 10 minutes. Surface biotin was stripped from the cells with a 10-minutes incubation in 50 mM MesNa. The cells were subsequently lysed, precipitated with 50% streptavidin-agarose beads, and subjected to Western blot analyses for EGFR. Whole cell lysates of each set were also extracted and subjected to Western blot analyses to confirm that there was difference in the total amount of EGFR between control and cetuximab-treatment groups. B) Expression of p-ERK and ERK in CCK-81 or Caco-2 cells. CCK-81 cells (sensitive to cetuximab) or Caco-2 cells (less sensitive to cetuximab) were treated with cetuximab at 30, 100, or 300 nM for 24 hours, respectively, and Western blotting for p-ERK and ERK was performed. β-actin was used as a loading control. C) Quantitative analysis of

Western blot data by densitometry. Western blot data were scanned by densitometry and analyzed using Image J software. The p-ERK signal was normalized to the corresponding total ERK signal and then set to 100% for untreated controls. Error bars show mean ± SD. *P*-values were determined using Student's t test. **p* <0.001. C) Expression of PARP and cleaved PARP in CCK-81 or Caco-2 cells. The cells were treated with cetuximab (100 nM) or vehicle for 5 days, and Western blotting for PARP and cleaved PARP was performed. β-actin was used as a loading control.

**Figure 5.**

Immunohistochemical analysis of EGFR expression in CRC tissue. A) The representative staining patterns of "marked decrease" (case 5, a-c), "moderate decrease" (case 12, d-f), and "no change" (case 9, g-i) in immunoreactivity for EGFR. a, d, g, H&E staining; b, e, h, before treatment; c, f, I, after treatment. Bar, 100 μm. B) Waterfall plots of best tumor response in CRC patients treated with anti-EGFR monoclonal antibody. Response was evaluated according to RECIST version 1.1. C) Correlation of EGFR immunoreactivity and response to anti-EGFR antibody. The numbers of patients in the "no change", "moderate decrease", and "marked decrease" categories were compared between responder and non-responder groups using the chi-square test.

**Table 1** Baseline characteristics of patients

| No. | Sex | Age | Location | Anti-EGFR mAbs | Tumor differentiation | Combination chemotherapy | Cycle | Time from last chemotherapy dose to tissue acquisition (days) |
|---|---|---|---|---|---|---|---|---|
| 1 | F | 66 | D | cetuximab | well differentiated type | FOLFIRI | 4 | 14 |
| 2 | M | 57 | R | cetuximab | well > moderately differentiated type | FOLFOX | 4 | 27 |
| 3 | M | 66 | S | cetuximab | moderately differentiated type | FOLFOX | 6 | 27 |
| 4 | M | 50 | S | cetuximab | moderately differentiated type | FOLFIRI | 5 | 33 |
| 5 | F | 45 | S | cetuximab | moderately differentiated type | FOLFOX | 4 | 41 |
| 6 | M | 72 | C | cetuximab | moderately differentiated type | IRI | 5 | 22 |
| 7 | M | 65 | R | cetuximab | moderately differentiated type | FOLFIRI | 6 | 20 |
| 8 | M | 60 | R | panitumumab | poorly differentiated type | FOLFOX | 3 | 99 |
| 9 | M | 70 | R | cetuximab | moderately differentiated type | FOLFIRI | 3 | 45 |
| 10 | F | 47 | S | cetuximab | well differentiated type | IRI | 7 | 16 |
| 11 | M | 36 | R | panitumumab | well differentiated type | FOLFOX | 7 | 28 |
| 12 | M | 72 | R | panitumumab | well differentiated type | IRIS | 2 | 34 |
| 13 | M | 64 | S | panitumumab | well differentiated type | IRIS | 4 | 25 |

M, male ; F, female ; C, cecum ; D, descending colon ; S, sigmoid colon ; R, rectum ;

mAbs, monoclonal antibodies ; FOLFIRI, irinotecan, leucovorin and fluorouracil ;

FOLFOX, oxaliplatin, leucovorin and fluorouracil ; IRI, irinotecan ; IRIS, irinotecan and S-1.

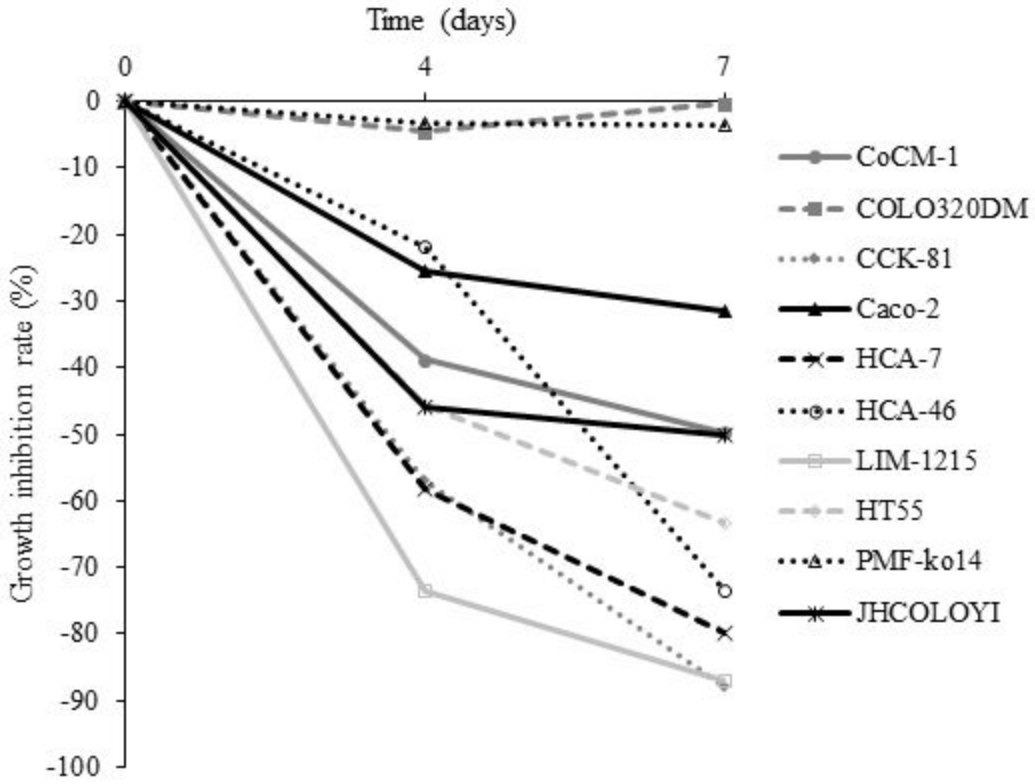
Time (days)
0
4
7
0
-10
-20
-30
-40
-50
-60
-70
-80
-90
-100
Growth inhibition rate (%)
CoCM-1
COLO320DM
CCK-81
Caco-2
HCA-7
HCA-46
LIM-1215
HT55
PMF-ko14
JHCOLOYI

Figure 1

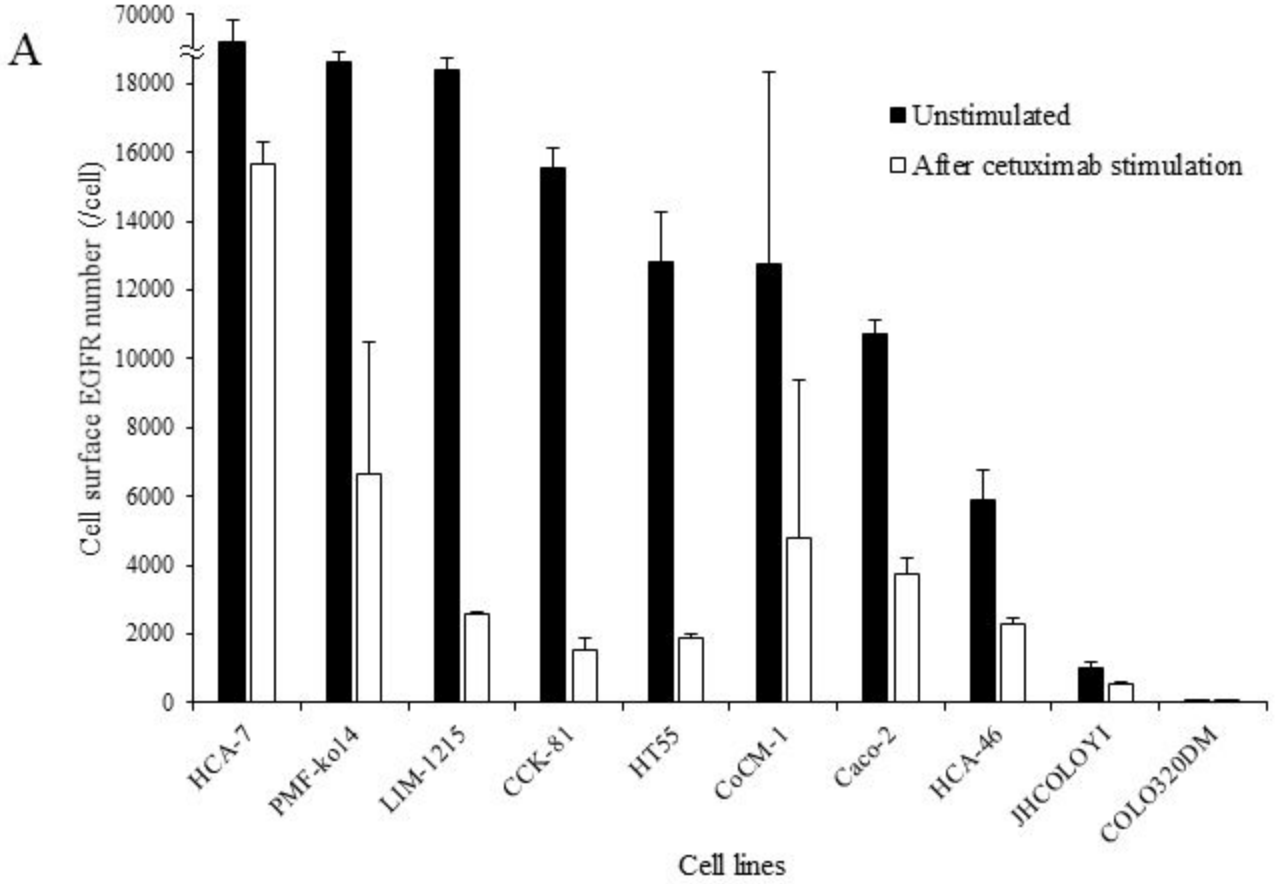
A
Cell surface EGFR number (/cell)
70000
18000
16000
14000
12000
10000
8000
6000
4000
2000
0
Unstimulated
After cetuximab stimulation
HCA-7
PMF-ko14
LIM-1215
CCK-81
HT55
CoCM-1
Caco-2
HCA-46
JHCOLOYI
COLO320DM
Cell lines

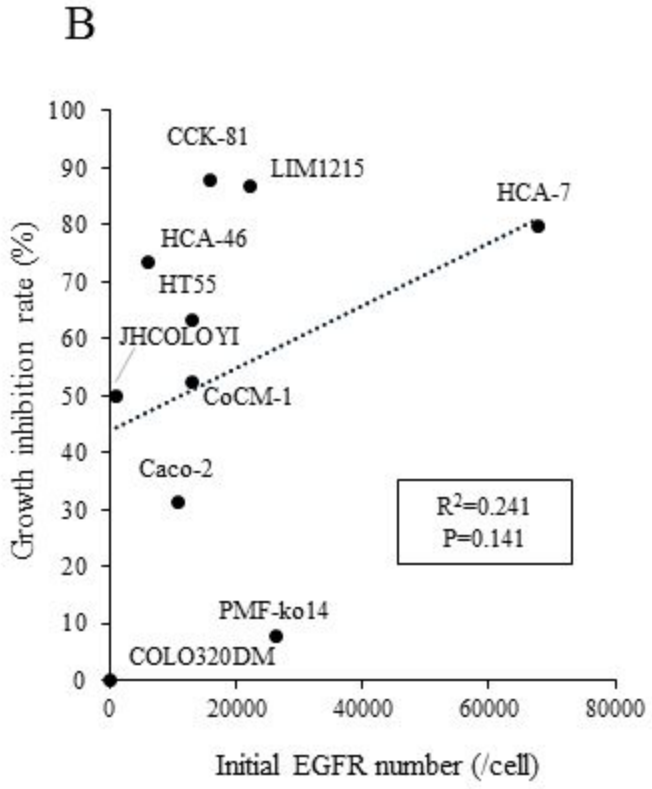
B
Growth inhibition rate (%)
100
90
80
70
60
50
40
30
20
10
0
CCK-81
LIM1215
HCA-7
HCA-46
HT55
JHCOLOYI
CoCM-1
Caco-2
PMF-ko14
COLO320DM
R2=0.241
P=0.141
0
20000
40000
60000
80000
Initial EGFR number (/cell)

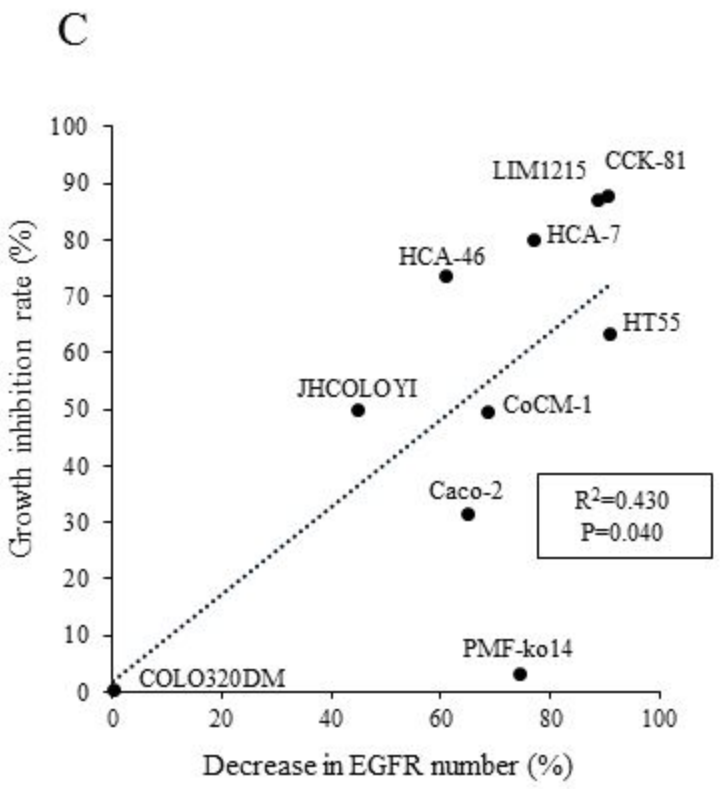
C
Growth inhibition rate (%)
100
90
80
70
60
50
40
30
20
10
0
LIM1215
CCK-81
HCA-7
HCA-46
HT55
JHCOLOYI
CoCM-1
Caco-2
PMF-ko14
COLO320DM
R2=0.430
P=0.040
0
20
40
60
80
100
Decrease in EGFR number (%)

Figure 2

Figure 3

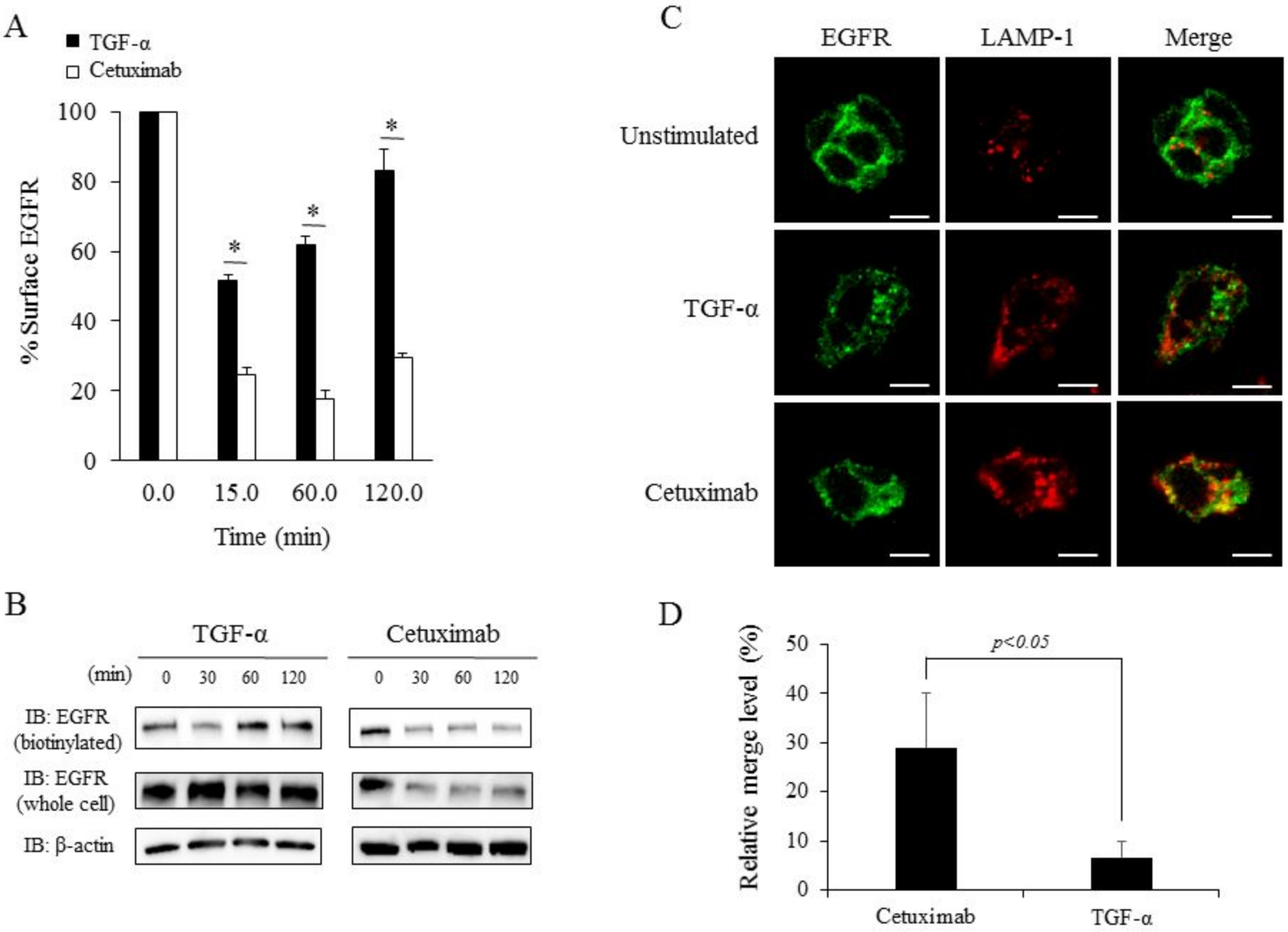
A
TGF-α
Cetuximab
% Surface EGFR
100
80
60
40
20
0
*
*
*
0.0
15.0
60.0
120.0
Time (min)
B
TGF-α
Cetuximab
(min)
0
30
60
120
0
30
60
120
IB: EGFR (biotinylated)
IB: EGFR (whole cell)
IB: β-actin
C
EGFR
LAMP-1
Merge
Unstimulated
TGF-α
Cetuximab
D
Relative merge level (%)
50
40
30
20
10
0
p<0.05
Cetuximab
TGF-α

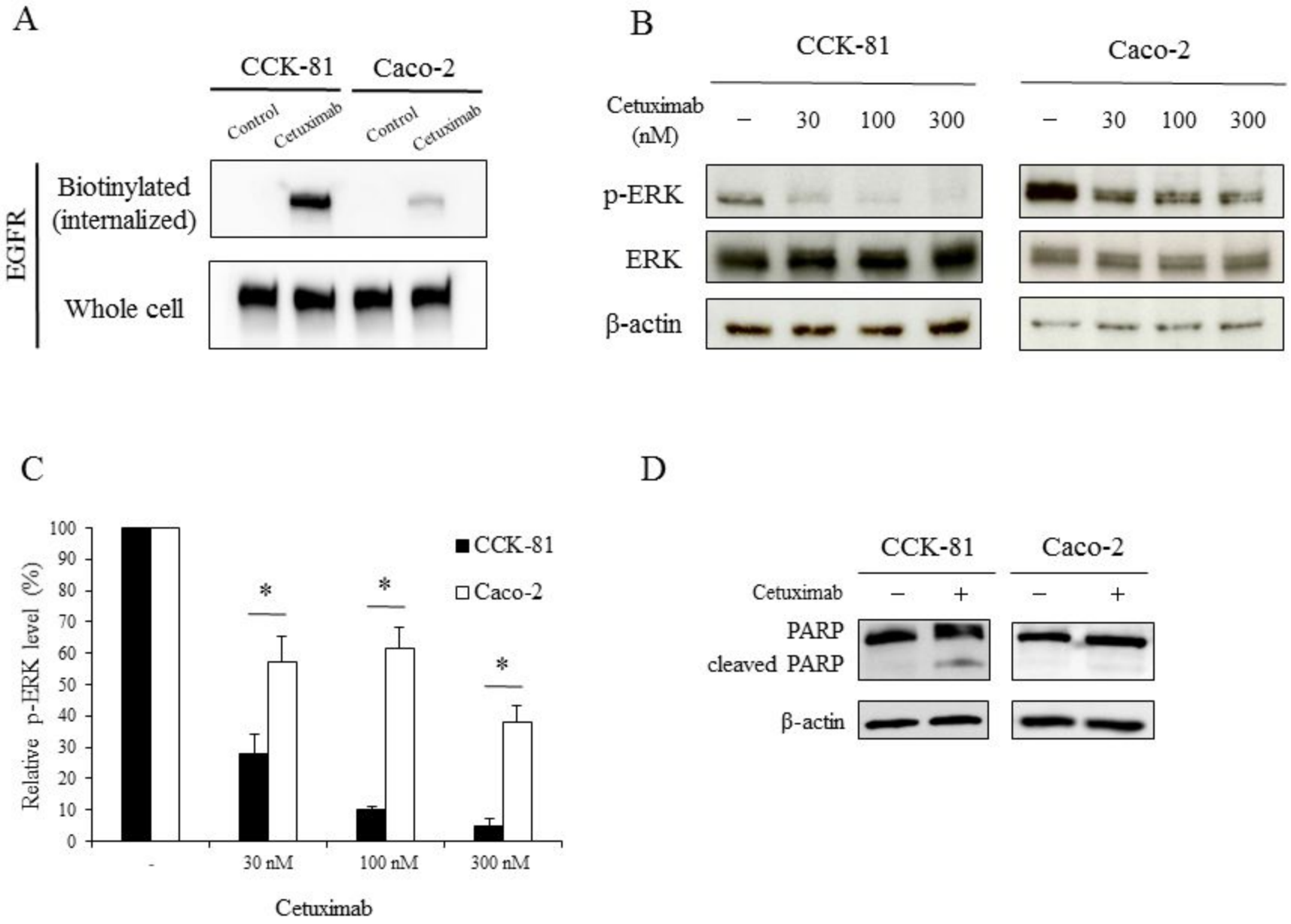
A
CCK-81
Caco-2
Control
Cetuximab
Control
Cetuximab
EGFR
Biotinylated (internalized)
Whole cell
B
CCK-81
Caco-2
Cetuximab (nM)
–
30
100
300
–
30
100
300
p-ERK
ERK
β-actin
C
Relative p-ERK level (%)
100
90
80
70
60
50
40
30
20
10
0
CCK-81
Caco-2
*
*
*
-
30 nM
100 nM
300 nM
Cetuximab
D
CCK-81
Caco-2
Cetuximab
–
+
–
+
PARP
cleaved PARP
β-actin

Figure 4

A

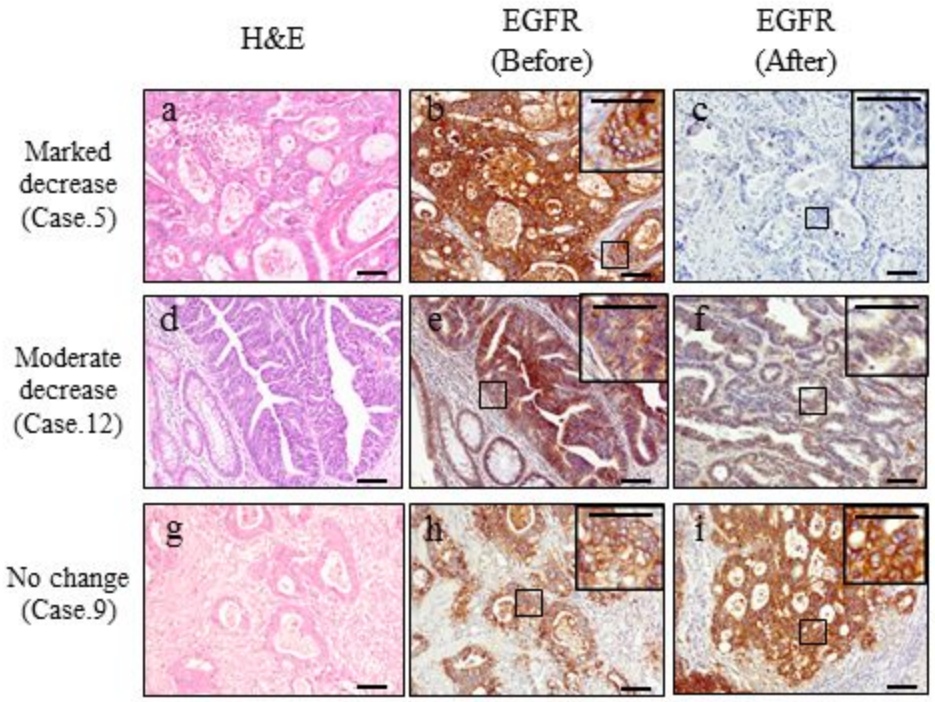


B

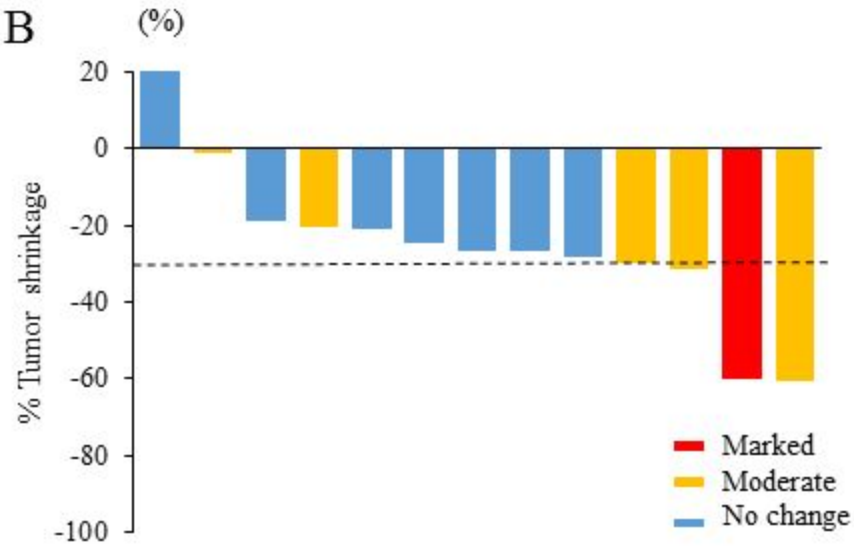


C

| | Patient | No change (%) | Moderate (%) | Marked (%) | |
|---|---|---|---|---|---|
| Responder | 4 | 0 (0) | 3 (75) | 1 (25) | $p < 0.01$ |
| Non-responder | 9 | 7 (78) | 2 (22) | 0 (0) | |

Figure 5